American Mineralogist, Volume 82, pages 740–747, 1997

$Mn_3Al_2Si_3O_{12}$ spessartine and $Ca_3Al_2Si_3O_{12}$ grossular garnet: Structural dynamic and thermodynamic properties

CHARLES A. GEIGER[1] AND THOMAS ARMBRUSTER[2]

[1]Mineralogisch-Petrographisches Institut der Christian-Albrechts-Universität zu Kiel, Olshausenstr. 40 D-24098 Kiel, Germany
[2]Laboratorium für chemische und mineralogische Kristallographie, Universität Bern, Freiestrasse 3, CH-3012 Bern, Switzerland

ABSTRACT

The structures of synthetic $Mn_3Al_2Si_3O_{12}$ spessartine and $Ca_3Al_2Si_3O_{12}$ grossular garnet have been refined using single-crystal X-ray diffraction methods at 100 K, 293 K, and 500-550 K. The divalent X-site cations, located in large dodecahedral sites, show measurable anisotropic dynamic disorder in contrast to the rigid vibrational behavior of the SiO_4 tetrahedra and AlO_6 octahedra. The amplitudes of vibration of Mn^{2+} in spessartine are similar to those of Fe^{2+} of almandine, in the plane of the longer X-O(4) bonds, and both are about twice that of Ca^{2+} in grossular, despite the lighter mass of the latter. Heat capacities measured between 300 and 1000 K on synthetic polycrystalline spessartine and two natural nearly end-member spessartine crystals are similar to those of almandine. In addition, the IR active modes of spessartine at low frequencies are very similar to those of almandine suggesting that their heat capacities are also similar at lower temperatures. The low-energy phonon spectra of pyrope and grossular are probably considerably distinct from the two transition metal-containing garnets as suggested by their different low frequency IR active modes, reflecting the different bonding properties for Mg and Ca in garnet. The large pressure-temperature stability field of spessartine, relative to the other aluminosilicate garnets, does not appear to be due to any sort of intrinsic entropy stabilization.

INTRODUCTION

The garnet group is extremely diverse showing a wide compositional range (e.g., Geller 1967). One class of garnet, the silicate garnets of space group $Ia\bar{3}d$ (Menzer 1928), which occur commonly in nature, are, in addition, thermodynamically stable over very large pressure and temperature regimes. They show, in comparison with most silicate structures, little in the way of phase transitions or instability as a function of pressure and temperature. The aluminosilicate garnets of the general formula $X_3Al_2Si_3O_{12}$, where for the most common end-members X = Fe^{2+} (almandine), Ca^{2+} (grossular), Mn^{2+} (spessartine), and Mg^{2+} (pyrope), are a good example for such phase stability. As a group, they are stable from 1 atm up to several 10s of GPa from roughly 400 °C to very high temperatures. The aluminosilicate garnets also possess the ability to form extensive solid solutions, as shown by the mixing of different cations on the dodecahedral X-site, Wycoff position 24(c).

The static structural description of garnet, largely based on room temperature diffraction experiments, is well known since its initial structure determination by Menzer (1928). Recently, the dynamic properties of the polyhedral units and the X-site cations of some of the end-member silicate garnets (almandine, pyrope, and andradite-$Ca_3Fe_2Si_3O_{12}$) have been investigated by temperature-dependent, X-ray single-crystal refinements between 100 and 500 K (Geiger et al. 1992; Armbruster et al. 1992; Armbruster and Geiger 1993). An analysis of the atomic mean-square difference displacement parameters (Bürgi 1989) as a function of temperature shows that the SiO_4 tetrahedra and the AlO_6 octahedra can be considered as rigid bodies over this temperature range, thus confirming the static polyhedral description of the structure (Zemann 1962). The divalent X-site cations show, in contrast, substantial anisotropic dynamic disorder in the large irregular dodecahedral site (Geiger et al. 1992; Armbruster et al. 1992; Armbruster and Geiger 1993). Recognition of this dynamic disorder allows new insight into the garnet structure and has enabled, for example, several unusual and previously not understood spectroscopic features to be elucidated (Geiger et al. 1992; Quartieri et al. 1997; Kolesov and Geiger, in press).

In addition, thermodynamic properties such as heat capacity could depend on the dynamic properties of the X-site cations. The relatively large heat capacity of pyrope at low temperatures (Haselton and Westrum 1980), for example, may be related to the large amplitude, low energy vibrations of the Mg cations. The phonon density of states of the silicate garnets are unknown. Only a few

dispersion curves for the acoustic phonons of pyrope were measured (Artioli et al. 1996) and hence, a rigorous analysis of the lattice dynamics of it or of the other silicate garnets is not possible.

We examine, herein, the structures of synthetic $Mn_3Al_2Si_3O_{12}$ spessartine and $Ca_3Al_2Si_3O_{12}$ grossular garnet between 100 and 500-550 K, as determined by single crystal X-ray refinements, and analyze the behavior of the X-site cations with respect to the temperature dependence of their amplitudes of vibration. The heat capacity of spessartine, which was previously unknown, is also presented between 300 to 1000 K and is compared with the heat capacities of the other aluminosilicate garnets. The powder FTIR spectra of the four synthetic aluminosilicate garnets between 450 and 80 cm^{-1} are also compared. Finally, the large *P-T* stability of spessartine is addressed in light of these new measurements.

Experimental methods

Inasmuch as nearly all natural garnets are compositionally complex solid solutions, it is necessary to synthesize end-member garnet compositions for the study of dynamic properties using X-ray diffraction. Static positional disorder resulting from localized compositional differences cannot be separated easily from true dynamical disorder, and therefore, end-member garnet compositions must be synthesized for these measurements. A short description of the synthesis methods used for the aluminosilicate garnets is given in Geiger et al. (1988).

The grossular single crystals used for X-ray study were synthesized hydrothermally at 1073 K and 0.2 GPa for a period of eight weeks from a fine-grained and intimately ground oxide mixture of CaO (from $CaCO_3$), SiO_2 (quartz), and Al_2O_3 (corundum) of stoichiometric grossular composition. Standard cold-seal vessels and associated methods were used. It is difficult to synthesize large crystals of grossular (greater than several hundred micrometers), and the largest crystals obtained were about 100 μm in diameter. Most of the synthesis product consisted of finer grossular crystals about 15 μm in diameter. Additional phases, which were not identified, were present at about 5–10 vol%.

It is also difficult to synthesize large spessartine single crystals. Attempts to grow large crystals hydrothermally using an oxide mixture of MnO, SiO_2, and Al_2O_3 or a glass of stoichiometric spessartine composition result in crystals of about 10–15 mm in size or smaller. Spessartine shows the lowest temperature stability of the aluminosilicate garnets (Hsu 1968), and it appears that rapid nucleation at low temperatures does not allow the growth of large single crystals. To hinder rapid nucleation and growth, a different synthesis method was adopted. A starting mixture consisting of Mn_2O_3, Al_2O_3, and SiO_2 was prepared. This mixture was sealed with distilled water in gold capsules and held at 1073 K and 0.2 GPa for a period of about one month. The oxidation state within the cold-seal hydrothermal vessels used is approximately that of the Ni-NiO buffer (Huebner 1971), and Mn_2O_3 is apparently slowly reduced to MnO during the experiment, and spessartine nucleation and subsequent growth proceeds in a slower fashion than when using MnO as a starting material. In this manner, spessartine crystals up to about 200 μm can be produced. Several types of crystals were observed. Large single crystals, somewhat rounded, showing {110} and {211} faces were found, as were more skeletal-like crystals having pointed projections atypical of the normal garnet habit. Similar crystals were documented in the work of Matthes (1961; see Fig. 7). The cores of most of the larger crystals are reddish orange in color, while the rims are generally more translucent and lighter orange. The darker color is probably attributable to small amounts of Mn^{3+} substituting for Al^{3+} in the octahedral site. A refinement of the unit-cell dimension, a_0, of this material based on a powder X-ray pattern between 20° and 120° 2θ, gave 11.618(1) Å, with the error representing 2σ statistics.

Polycrystalline spessartine was also synthesized anhydrously at high pressures and temperatures for heat capacity measurements. First, a glass of stoichiometric spessartine composition was prepared by melting MnO, SiO_2, and Al_2O_3 in a graphite capsule at 1523 K and then quenching in water. About 200 mg of finely ground glass, without water, was welded into a platinum capsule of 5 mm diameter and crystallized at 1273 K and 1.6 GPa in a piston-cylinder device. The resulting synthesis product was better than 99.5% spessartine and gave an a_0 cell dimension of 11.6163 (5), Å based on a least-squares refinement of a powder X-ray pattern, using NBS 640b Si as an internal standard, in the range between 10–135° 2θ. [The cell dimension of spessartine depends on OH^- content for those synthesized hydrothermally at low temperatures and probably on the amount of Mn^{3+}. Geiger et al. (1988) considered the value a_o = 11.615(1) the best estimate for end-member stoichiometric spessartine.]

Heat-capacity measurements on spessartine were made using an automated Perkin Elmer DSC 7 differential scanning calorimeter (Watson et al. 1964). The experimental methods adopted are identical to those reported in Bosenick et al. (1996). The step-scanning technique was used and machine stability and accuracy was checked by measuring the heat capacity of single crystal MgO. Measurements were made on the synthetic polycrystalline spessartine and, in addition, on two natural spessartine single crystals obtained from G.R. Rossman (California Institute of Technology). The first sample, labeled GRR 43b, is from the Rutherford no. 2 Mine in Amelia, Virginia. The second, labeled GRR 1791, is from an unknown location in Namibia. The chemical composition of both natural spessartine crystals was determined by electron microprobe analysis, and the results are given in Table 1. The Rutherford spessartine is light orange, while that from Namibia is slightly darker in color. Both are translucent and optically free of included phases. Both crystals were cut and polished on opposite sides giving single crystal platelets. The former single crystal is about 4 × 5.5 mm in cross section and about 1.50 mm thick

TABLE 1. Chemical analyses of the natural spessartine crystals used in the DSC measurements

Sample	43b	1791
	Wt% oxides	
SiO_2	36.10	37.03
TiO_2	00.01	00.18
Al_2O_3	20.68	19.37
Cr_2O_3	00.01	00.03
FeO	01.23	01.68
MnO	41.89	39.06
MgO	00.00	2.44
CaO	00.73	00.78
Na_2O	00.00	00.02
Total	100.65	100.57
Si	2.97	3.00
Ti	0.00	0.01
	Cations per 12 O atoms	
Al	2.00	1.85
Cr	0.00	0.00
Fe^{3+}	0.00	0.12
Fe^{2+}	0.08	0.00
Mn	2.91	2.68
Mg	0.00	0.29
Ca	0.06	0.07
Sum	8.02	8.02
O atoms	12	12
X_{spess}	0.97	0.89
X_{almd}	0.02	0.00
X_{py}	0.00	0.09
$X_{gross/and}$	0.01	0.02

and weighs 50.81 mg. The latter is about 3.5 × 5 mm and about 2 mm thick and weighs 55.23 mg. Sample 43b was measured once with a heating rate of 10 °C/min and the other two spessartines were measured at 10 and 20 °C/min, wherein the two measurements were averaged.

Powder FTIR spectra of the four synthetic aluminosilicate garnet end-members (pyrope, almandine, grossular, and spessartine) were recorded using a Bruker spectrometer by imbedding about 1 to 2 mg of ground garnet in polyethylene and pressing into pellets. A total of 32 scans measured at a resolution of 2 cm^{-1} were recorded. A single crystal IR measurement, on a grossular crystal of about 100 micrometer size (Fig. 1), synthesized hydrothermally, was made using a Nicolet spectrometer in the laboratory of G.R. Rossman at Caltech using the methods described in Geiger et al. (1991).

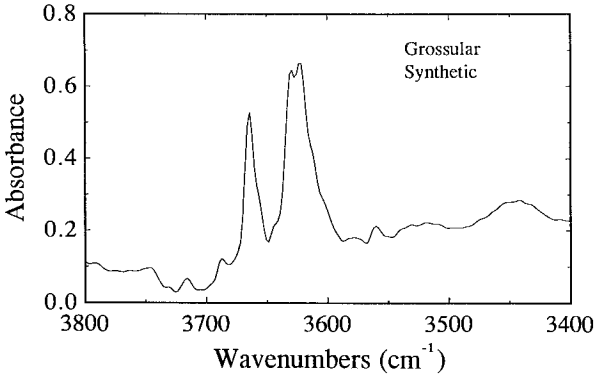

FIGURE 1. Single-crystal FTIR spectrum of grossular between 3800 and 3400 cm^{-1}. The spectrum is normalized to 1 mm thickness. This energy region is characterized by OH^- stretching vibrations of structurally bound OH^- groups in the garnet structure.

TABLE 2A. Experimental conditions used in the single crystal data collection for spessartine of size 0.300 × 0.220 × 0.180 mm

Temperature	100 K	293 K	500 K
Unit-cell dimension	11.606(1)	11.619(1)	11.641(1)
θ range	<50°	<50°	<50°
scan type (ω-2θ)	2.5°	2.5°	2.5°
No. measured reflections	1456	1454	1352
R_{int}(I), (%)	1.5	1.4	1.3
No. unique reflections	502	503	506
No. reflections with sinθ/λ > 0.4 and $F_{obs} > 6\sigma(F_{obs})$	351	308	242
No. parameters	18	18	18
R (%)	1.9	2.0	1.5
R_w (%)	2.0	2.2	1.6

The X-ray single-crystal data were collected up to at least θ = 30° of one complete octant in reciprocal space on an Enraf Nonius CAD4 single-crystal diffractometer with graphite monochromated Mo$K\alpha$ radiation. An exception are the 293 K grossular data, which were obtained on a Siemens P4R diffractometer, also using graphite monochromated Mo$K\alpha$ radiation, equipped with a rotating anode (50 kV, 150 mA). Intensities between θ = 30 and 50° were collected only for those reflections for which tests indicated significant intensity. Low temperature measurements (100 ± 5 K) were made with a conventional liquid nitrogen cooling device. For the collection of the 500-550 ± 10 K data sets a self-constructed regulated hot-air blower was used. Reflection intensities were empirically corrected for absorption by using Ψ scans. The data collection (assuming I centering) and refinement procedures are similar to those described in Geiger et al. (1992) and Armbruster et al. (1992). Additional details are given in Table 2. Only reflections with $\sin\theta/\lambda > 0.4$, weighed $1/\sigma^2$, were considered in the spessartine refinements using the program PROMETHUS (Zucker et al. 1983). In the case of grossular structure refinements, the program SHELXTL (Siemens 1990) was

TABLE 2B. Experimental conditions used in the single crystal data collection for grossular of size 0.125 × 0.125 × 0.100 mm

Temperature	100 K	293 K	550 K
Unit-cell dimension	11.837(1)	11.847(1)	11.872(1)
θ range	<50°	<50°	<50°
scan type (ω-2θ)	1.0°	1.0°	1.0°
No. measured reflections	1779	1424	3276
R_{int}(I), (%)	2.1	2.8	2.3
No. unique reflections	484	566	640
No. reflections with sinθ/λ > 0.4 and $F_{obs} > 6\sigma(F_{obs})$	319	383	232
No. parameters	18	18	18
R (%)	1.6	2.5	1.4
R_w (%)	1.9	3.3	1.8

Note: $R = \Sigma\big||F_{obs}| - |F_{calc}|\big|/\Sigma|F_{obs}|$, $R_w = (\Sigma w(|F_{obs}|) - |F_{calc}|)^2/\Sigma w|F_{obs}|^2)$

TABLE 3. Positional and displacement parameters of synthetic grossular between 100 and 550 K

	Grossular 100 K	Grossular 293 K	Grossular 550 K
	Oxygen		
X	0.03823(6)	0.03823(7)	0.03839(7)
Y	0.04542(6)	0.04528(7)	0.04483(8)
Z	0.65125(5)	0.65137(6)	0.65142(7)
B_{eq}	0.263(7)	0.411(9)	0.63(1)
U_{11}	0.0034(2)	0.0049(3)	0.0077(3)
U_{22}	0.0040(2)	0.0063(3)	0.0095(3)
U_{33}	0.0026(2)	0.0044(2)	0.0066(3)
U_{12}	0.0000(2)	0.0002(2)	0.0009(2)
U_{13}	−0.0005(2)	−0.0005(2)	−0.0009(2)
U_{23}	0.0001(2)	0.0004(2)	0.0002(2)
	X cation (0, ¼, ⅛); $U_{11} = U_{22}$, $U_{13} = U_{23} = 0$		
B_{eq}	0.212(3)	0.445(5)	0.708(4)
U_{11}	0.00296(8)	0.0064(1)	0.0104(1)
U_{33}	0.0021(1)	0.0042(1)	0.0062(1)
U_{12}	0.0003(1)	0.0010(1)	0.0020(1)
	Y cation (0, 0, 0); $U_{11} = U_{22} = U_{33}$, $U_{12} = U_{13} = U_{23}$		
B_{eq}	0.194(3)	0.365(4)	0.527(3)
U_{11}	0.00246(9)	0.0046(1)	0.0067(1)
U_{12}	−0.0000(1)	−0.0001(1)	−0.0001(2)
	Si (⅜, 0, ¼); $U_{22} = U_{33}$, $U_{12} = U_{13} = U_{23} = 0$		
B_{eq}	0.175(4)	0.328(6)	0.425(6)
U_{11}	0.0022(2)	0.0040(2)	0.0051(2)
U_{22}	0.0022(1)	0.0042(1)	0.0055(2)

TABLE 4. Positional and displacement parameters of synthetic spessartine between 100 and 500 K

	Spessartine 100 K	Spessartine 293 K	Spessartine 500 K
	Oxygen		
X	0.03493(6)	0.03491(7)	0.03508(6)
Y	0.04816(6)	0.04791(7)	0.04744(6)
Z	0.65246(6)	0.65250(7)	0.65237(6)
B_{eq}	0.243(7)	0.354(7)	0.583(8)
U_{11}	0.0031(2)	0.0044(2)	0.0072(2)
U_{22}	0.0038(2)	0.0055(2)	0.0094(3)
U_{33}	0.0023(2)	0.0036(2)	0.0055(2)
U_{12}	0.0005(2)	0.0010(2)	0.0008(2)
U_{13}	−0.0006(2)	−0.0010(2)	−0.0015(2)
U_{23}	−0.0002(2)	0.0001(2)	0.0001(2)
	X cation (0, ¼, ⅛); $U_{11} = U_{22}$, $U_{13} = U_{23} = 0$		
B_{eq}	0.231(2)	0.486(3)	0.861(3)
U_{11}	0.00345(7)	0.0076(1)	0.0134(1)
U_{33}	0.0019(1)	0.0033(1)	0.0059(1)
U_{12}	0.00058(8)	0.0026(1)	0.0029(1)
	Y cation (0, 0, 0); $U_{11} = U_{22} = U_{33}$, $U_{12} = U_{13} = U_{23}$		
B_{eq}	0.181(2)	0.254(2)	0.419(2)
U_{11}	0.0023(1)	0.0032(1)	0.0053(1)
U_{12}	0.0002(1)	0.0000(1)	−0.0000(1)
	Si (⅜, 0, ¼); $U_{22} = U_{33}$, $U_{12} = U_{13} = U_{23} = 0$		
B_{eq}	0.150(3)	0.214(4)	0.361(4)
U_{11}	0.0017(2)	0.0023(2)	0.0041(1)
U_{22}	0.0020(1)	0.0029(1)	0.0048(1)

used and reflections were weighed according to $W = H/[\sigma^2(F) + 0.0002F^2]$, where $H = 1 - \exp[-5(\sin\theta/\lambda)^2]$. The H term yields a larger contribution to the high angle reflections. Thus, in contrast to the spessartine data set, no low angle $\sin\theta/\lambda$ cutoff was applied. The use of the two different refinement programs was only done for technical reasons and does not effect the resulting refined parameters. The refinements used high-angle data, thus leading to more precise atomic coordinates and atomic-displacement parameters, which are necessary for the study of dynamic properties.

RESULTS

The single-crystal IR spectrum of a hydrothermally grown grossular crystal between 3800 and 3400 cm^{-1} is shown in Figure 1. It is different from that given by $Ca_3Al_2(O_4H_4)_3$ katoite, where the OH^- groups build a O_4H_4-tetrahedron (Cohen-Addad et al. 1967). The former shows at least three OH^- stretching vibrations, which cannot be assigned to definite structural positions. It is most similar to the ''class 4'' type of natural grossular described by Rossman and Aines (1991). Using their calibration for OH^- contents in H_2O-containing grossular, we calculate roughly 0.04 wt% H_2O for this synthetic grossular.

The refined O coordinates and the anisotropic displacement parameters for all the atoms in grossular and spessartine at the three temperatures of 100, 293, and 500–550 K are listed in Tables 3 and 4, respectively. The structural parameters (i.e., bond lengths and angles) at 293 K are similar, but not exactly the same as those reported on a natural spessartine-rich garnet by Novak and Gibbs (1971) and those from natural nearly end-member grossulars by Abrahams and Geller (1958), Prandl (1966), and Novak and Gibbs (1971). Meagher (1975) refined the structure of a natural grossular at temperatures of 293, 638, and 948 K. The four crystallographically independent cation-oxygen bond lengths at the three different temperatures are given in Table 5.

Table 6 lists the difference displacement parameters, ΔUs (Bürgi 1989), for both grossular and spessartine at the three temperatures. As in the case of pyrope and almandine (Armbruster et al. 1992), the ΔUs along the Si-O and Al-O bonding vectors do not change measurably as a function of temperature. The two crystallographically independent X-O bonds show different behavior as a function of temperature. The ΔUs along the bonding vector X-O(2) do not change with increasing temperature, whereas the ΔUs associated with the X-O(4) bonds increase measurably.

TABLE 5. Cation-oxygen bond distances in spessartine and grossular

T (K)	Si-O (Å)	Al-O (Å)	X-O(2) (Å)	X-O(4) (Å)
		Spessartine		
100	1.639(1)	1.899(1)	2.245(1)	2.399(1)
293	1.640(1)	1.901(1)	2.246(1)	2.404(1)
500	1.641(1)	1.902(1)	2.251(1)	2.414(1)
		Grossular		
100	1.646(1)	1.923(1)	2.321(1)	2.483(1)
293	1.646(1)	1.926(1)	2.322(1)	2.487(1)
550	1.646(1)	1.929(1)	2.322(1)	2.498(1)

TABLE 6. Difference mean-square-displacement parameters [$\Delta U = U_{cation} - U_{oxygen}$ (Å²)] evaluated along the four bonding vectors in spessartine and grossular

T (K)	Si-O (Å²)	Al-O (Å²)	X-O(2) (Å²)	X-O(4) (Å²)
		Spessartine		
100	−0.0003(2)	−0.0001(2)	−0.0014(2)	0.0000(2)
293	−0.0002(2)	−0.0003(2)	−0.0015(2)	0.0030(2)
500	−0.0004(2)	−0.0002(2)	−0.0010(2)	0.0054(2)
		Grossular		
100	−0.0003(2)	−0.0001(2)	−0.0014(2)	−0.0008(2)
293	−0.0000(3)	0.0001(3)	−0.0007(3)	0.0007(3)
550	−0.0007(3)	−0.0002(3)	−0.0015(3)	0.0021(3)

The heat capacity results for the different spessartines are plotted in Figure 2. The heat capacities of the two natural spessartines are slightly greater than those of the synthetic. Fitted C_p polynomials of the type recommended by Berman (1988) in the temperature range from 300 to 1000 K for synthetic spessartine and the two natural spessartines (GRR 43b and 1791), respectively, are as follows (T in Kelvins and C_p in J/mol·K):

$$C_p = 547.33 - 852.99T^{-0.5} - 31.544 \times 10^6 T^{-2} + 5240.40 \times 10^6 T^{-3} \quad (1)$$

$$C_p = 631.07 - 4051.56T^{-0.5} - 55.516 \times 10^6 T^{-2} - 4875.71 \times 10^6 T^{-3} \quad (2)$$

$$C_p = 576.4 - 2113.88\ T^{-0.5} - 16.059 \times 10^6 T^{-2} + 1749.02 \times 10^6 T^{-3} \quad (3)$$

The C_p values of the three different samples are within 1% of each other at temperatures between 600 and 1000 K, while at lower temperatures they differ by about 2%. The powder FTIR spectra of the four synthetic aluminosilicate garnets between 450 and 80 cm^{-1} are shown in Figure 3.

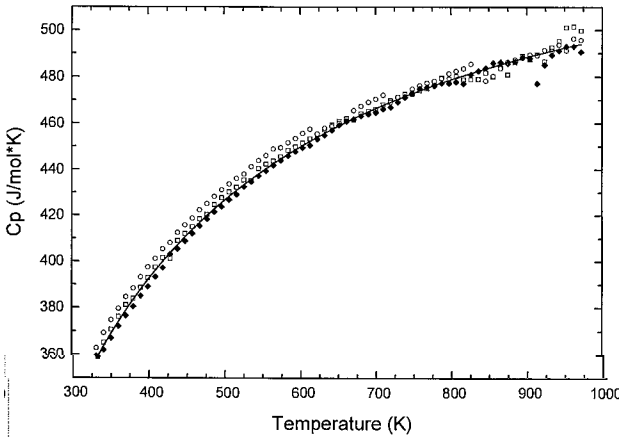

FIGURE 2. Heat capacities of the three spessartine samples measured between 320 and 1000 K. The squares represent the natural sample 43b, the circles natural sample 1791, and the diamonds synthetic spessartine. Least-squares best fit C_p polynomials to the data are given in the text. The solid line represents the calculated C_p of spessartine as deduced by static lattice energy calculations (Ottonello et al. 1996).

DISCUSSION

Crystal chemistry and bonding

The static description of the silicate garnet structure is well known (e.g., Menzer 1928; Novak and Gibbs 1971; Merli et al. 1995). The results, herein, permit a further analysis of the dynamic vibrational properties, especially of the X-site cations, and a comparison with the other silicate garnets almandine, pyrope, and andradite (Geiger et al. 1992; Armbruster et al. 1992; Armbruster and Geiger 1993). An analysis of the ΔU parameters (Table 6) shows that, as in the other silicate garnets, the SiO_4 tetrahedra and the AlO_6 octahedra in spessartine and grossular can be considered as rigid bodies between 100 and 500-550 K, inasmuch as the ΔU values associated with both polyhedra remain constant as a function of temperature. The vibrations of both polyhedra can be described by external librational and translational motions (see Armbruster and Geiger 1993).

The Mn^{2+} and Ca^{2+} cations show measurable dynamic disorder in the plane of the longer X-O(4) bonds of the dodecahedral site of point symmetry 222. This is evidenced by the change in their corresponding ΔU parameters from 100 to 500-550 K. In contrast, the ΔU parameters do not change along the bonding vector X-O(2). Hence, most of the X-site cation motion is within the plane defined by the four longer X-O(4) bonds. A graphical display of this disorder can be made by using of the program PEANUT (Hummel et al. 1991). Figure 4 shows the differences in the mean-square displacements between 500-550 and 100 K for the Mn^{2+} and Ca^{2+} cations in spessartine and grossular, respectively. The amplitudes of vibration for Mn^{2+} in spessartine are similar to those of

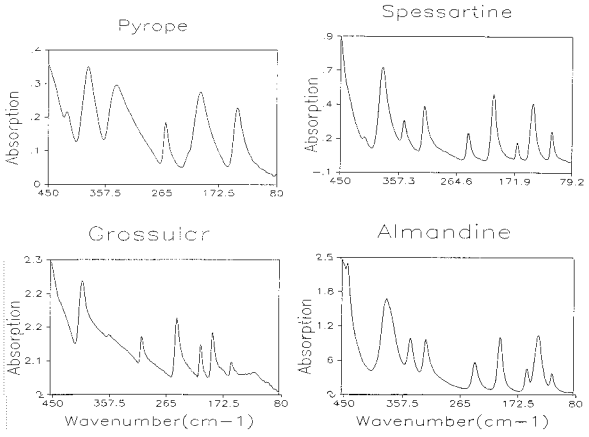

FIGURE 3. Powder FTIR spectra of synthetic spessartine, almandine, pyrope, and grossular between 450 and 100 cm^{-1}. The mode assignments and frequencies for almandine and spessartine are listed in Table 7.

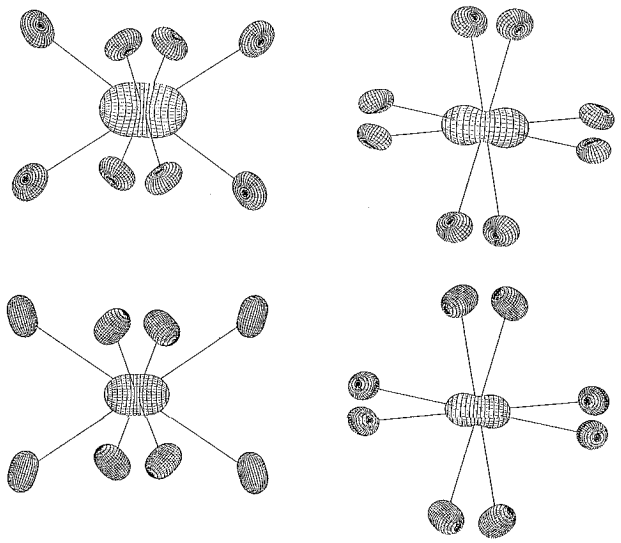

FIGURE 4. Differences of the atomic mean-square displacements (msd scale:64) between 500–550 and 100 K for Mn^{2+} in spessartine (above) and Ca^{2+} in grossular (below) (illustrated using the program PEANUT-Hummel et al. 1991). The projections are approximately along twofold axes. The projections on the right are rotated approximately 90° around the horizontal line of the projection in the left column. The X-cations show substantial anisotropic vibrational disorder, while the eight surrounding O anions show little disorder.

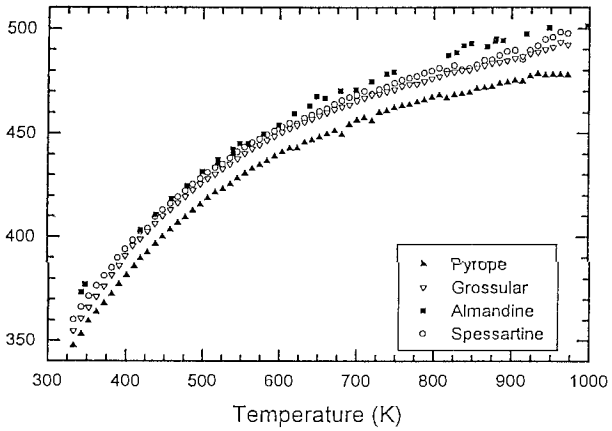

FIGURE 5. Comparison plot of the C_p values of the four synthetic end-member aluminosilicate garnets between 300 and 1000 K. The data for pyrope and grossular are from Bosenick et al. (1996), for almandine from Anovitz et al. (1992), and for spessartine from this study.

Fe^{2+} in almandine (Geiger et al. 1992; Armbruster et al. 1992). Both cations are of similar size in eightfold coordination (0.96 vs. 0.92 Å, respectively; Shannon 1976) and mass (54.94 and 55.85 a.m.u.). The main difference between Mn^{2+} and Fe^{2+} is in their respective electronic configurations. Mn^{2+} has five d electrons and Fe^{2+} six d electrons. Almandine garnet obtains, therefore, a crystal field stabilization energy (CFSE) from the additional electron in one of the lower e_g orbitals of Fe^{2+}. This may result in special bonding properties in the Fe^{2+} dodecahedral site and could be a possible explanation for the small differences observed in the vibrational amplitudes of Fe^{2+} relative to the other X-site cations as seen in PEANUT plots (see Armbruster and Geiger 1993). A description of the CFSEs for solid solutions between spessartine and almandine and their dodecahedral site distortions is given in Geiger and Rossman (1994). Ca^{2+} has, in contrast, no d electrons, and it is considerably larger than either Fe^{2+} and Mn^{2+}. It has a radius of 1.12 Å in eightfold coordination (Shannon 1976) and is also lighter than either of these two transition metals. It shows considerably smaller amplitude, roughly one-half, of vibration in the plane of the X-O(4) bonds than either Fe^{2+} or Mn^{2+}. Hence, the amplitudes of vibration of the X-site cations in garnet are not just a function of mass but also of size.

Thermodynamic properties and pressure-temperature stability of spessartine

The four aluminosilicate garnets show considerable differences in their pressure-temperature stabilities. Structural changes, resulting from the substitution of different X-site cations, certainly play a role in governing their thermodynamic stabilities. A question of interest concerns the large stability field of spessartine relative to the other garnets. Spessartine is stable at 1 atm and has its own liquidus surface in the system $MnO\text{-}Al_2O_3\text{-}SiO_2$ (Snow 1943). For the other aluminosilicate garnets this is not the case. In addition, spessartine has a very large *P-T* stability field in comparison with the three other aluminosilicate garnets, and unlike them, it melts congruently over a large *P-T* range (Mottana 1974). Almandine, though structurally very similar to spessartine, melts incongruently, and has a more restricted *P-T* stability field. Spessartine also shows a significantly larger thermal expansion in the temperature range from 273 K to 573 K compared to the other silicate garnets (Skinner 1956). A question to be asked is whether spessartine could gain its *P-T* stability through entropy stabilization. The relevant thermodynamic equation for the Gibbs free energy at 1 bar is:

$$\Delta G = \Delta H - T\Delta S \tag{4}$$

where, H is the enthalpy and S the entropy. The vibrational entropy is obtained by means of the heat capacity:

$$S_T = \int_{T=0}^{T} \frac{C_p}{T}\,\mathrm{d}T \tag{5}$$

Because spessartine and almandine are the most similar structurally, it is worthwhile to compare their heat capacities. Between 300 and 1000 K they are very similar, being within 1–2% of one another (Fig. 5). If they are different, than it should be in the low temperature region where they show the largest differences. A direct comparison of their heat capacities below 293 K is not possible however, because low-temperature heat capacity data for spessartine are not available.

They can be analyzed qualitatively, however, from the

TABLE 7. IR mode symmetries, assignments, and frequencies of spessartine and almandine garnet

Mode symmetry*	Mode assignment*	Spessartine (cm^{-1})	Almandine (cm^{-1})
T_{1u}	T(Al)	470	470
T_{1u}	ν_2	447	450
T_{1u}	R(SiO_4)	381	375
T_{1u}	R(SiO_4)	347	340
T_{1u}	T(SiO_4)	314	315
T_{1u}	T(Al)	243	237
T_{1u}	T(X)	204	197
T_{1u}	T(X)	166	154
T_{1u}	T(X)	140	136
T_{1u}	T(SiO_4)mix	111	114

* After Hofmeister and Chopelas (1991).

lattice dynamic properties of both phases as determined from the X-ray scattering experiments and their IR spectra. The root-mean-square value for an atomic displacement parameter can be written in the general harmonic case for an atom $u(j)$, in a monoatomic unit-cell as:

$$\langle |u(j)|^2 \rangle = \frac{3k_B T}{m_j \omega^2} \quad (6)$$

where k_B is Boltzmann's constant, ω the angular frequency and m_j the mass (Dove 1993).

The difference between the mass of Mn^{2+} and Fe^{2+} is about 2%, while the differences between the magnitude of their isotropic displacement parameters, B_{eq}, is at 293 K and 100 K only slightly greater [0.486(2) vs. 0.462(3) $Å^2$] and [0.231(2) vs. 0.215(1) $Å^2$; Geiger et al. 1992], respectively. The large U_{11} values in both are also very similar, while U_{33} and U_{12} are different, reflecting their smaller values and, therefore, uncertainties. Hence, application of Equation 6 suggests that the phonons related to Fe^{2+} and Mn^{2+} in almandine and spessartine, respectively, should be similar in energy assuming that the tetrahedral-octahedral framework is largely passive in terms of X-site cation vibrations (i.e., no strong mode coupling or mixing occurs) and that this simple-lattice dynamic model is applicable to the more complicated structure and dynamics of garnet.

This analysis can be tested through a comparison of the powder FTIR spectra of almandine and spessartine in the low wavenumber region (Fig. 3). Mode assignments and frequencies are given in Table 7. It should be stated, however, that some mode coupling is present between the IR modes in garnet (Cahay et al. 1981), and strict assignments to specific atomic or polyhedral motions is not possible. The X-site translation modes in both garnets are similar in frequency and in intensity, with the translation frequencies of Fe^{2+} being 3–7% lower than those of Mn^{2+}. The FTIR spectra of pyrope and grossular are, however, different from those of almandine and spessartine (Fig. 3), reflecting the different bonding properties and dynamical behavior of their X-site cations. Because their low frequency spectra are similar, the heat capacities of spessartine and almandine may also be similar at low temperatures, as it is the low-frequency optic modes that contribute greatly to the heat capacities at temperatures around 100 K (e.g., Born and Huang 1954). It is around this temperature where the heat capacity of pyrope is so large (Haselton and Westrum 1980). At temperatures between 300 and 1000 K, the heat capacities of the two garnets are very similar (Fig. 5). We expect, therefore, that their vibrational entropies will be similar at temperatures at least up to 1000 K.

In conclusion, it does not appear that spessartine possesses an abnormally large vibrational entropy, which could be invoked to explain its relatively large *P-T* stability field and stability at 1 atm in comparison with the other aluminosilicate garnets and especially to structurally similar almandine. Low-temperature C_p measurements on spessartine are now needed to test this hypothesis critically.

ACKNOWLEDGMENTS

We would like to thank Anne Bosenick for making the heat-capacity measurements and George R. Rossman for placing his IR lab at our disposal and for the donation of the natural spessartine crystals. Björn Winkler read the manuscript and suggested helpful changes. This research was supported by grant Ge 659/3-1 from the German Research Society.

REFERENCES CITED

Abrahams, S.C. and Geller, S. (1958) Refinement of the structure of a grossularite garnet. Acta Crystallographica, 11, 437–441.

Armbruster, T. and Geiger, C.A. (1993) Andradite crystal chemistry, dynamic X-site disorder and structural strain in silicate garnets. European Journal of Mineralogy, 5, 59–71.

Armbruster, T., Geiger, C.A., and Lager, G.A. (1992) Single-crystal X-ray structure study of synthetic pyrope almandine garnets at 100 and 293 K. American Mineralogist, 77, 512–521.

Anovitz, L.M., Essene, E.J., Metz, G.W., Bohlen, S.R., Westrum, E.F., Jr., and Hemingway, B.S. (1993) Heat capacity and phase equilibria of almandine, $Fe_3Al_2Si_3O_{12}$. Geochimica et Cosmochimica Acta, 57, 4191–4204.

Artioli, G., Pavese, A., and Moze, O. (1996) Dispersion relations of acoustic phonons in pyrope garnet: Relationship between vibrational properties and elastic constants. American Mineralogist, 81, 19–25.

Berman, R.G. (1988) Internally consistent thermodynamic data for minerals in the system Na_2O-K_2O-CaO-MgO-FeO-Fe_2O_3-Al_2O_3-SiO_2-TiO_2-H_2O-CO_2. Journal of Petrology, 29, 445–522.

Born, M. and Huang, K. (1954) Dynamical Theory of Crystal Lattices. Oxford University Press, London.

Bosenick, A., Geiger, C.A., Schaller, T., and Sebald, A. (1995) A ^{29}SiMAS NMR and IR spectroscopic investigation of synthetic pyrope-grossular garnet solid solutions. American Mineralogist, 80, 691–704.

Bosenick, A., Geiger, C.A., and Cemic, L. (1996) Heat capacity measurements of synthetic pyrope-grossular garnets between 320 and 1000 K by Differential Scanning Calorimetry. Geochimica et Cosmochimica Acta, 60, 3215–3227.

Bürgi, H.B. (1989) Interpretation of atomic displacement parameters: Intramolecular translational oscillation and rigid-body motion. Acta Crystallographica, B45, 383–390.

Cahay, R., Tarte, P., and Fransolet, A.-M. (1981) Interprétation du spectre infrarouge de variétés isotopiques de pyropes synthétiques. Bulliten de Minèralogie, 104, 193–200.

Cohen-Addad, P.C., Ducros, P., and Bertaut, E.F. (1967) Étude de la substitution du groupement SiO_4 par $(OH)_4$ dans les composés $Al_2Ca_3(OH)_{12}$ et $Al_2Ca_3(SiO_4)_{2.16}(OH)_{3.16}$ de type Granat. Acta Crystallographica, 23, 220–230.

Dove, M.T. (1993) Introduction to lattice dynamics. 258 p. Cambridge University Press, Cambridge.

Geiger, C.A. and Rossman, G.R. (1994) Crystal field stabilization energies

of almandine-pyrope and almandine-spessartine garnets determined by FTIR near infrared measurements. Physics and Chemistry of Minerals, 21, 516–525.

Geiger, C.A., Langer, K., Winkler, B., and Cemic, L. (1988) The synthesis, characterization and physical properties of end-member garnets in the system $(Fe,Mg,Ca,Mn)_3Al_2(SiO_4)_3$. In H. Vollstädt, Ed., High pressure geosciences and material synthesis, p. 193–198. Akademie-Verlag, Berlin.

Geiger, C.A., Langer, K., Bell, D.R., Rossman, G.R., and Winkler, B. (1991) The hydroxide component in synthetic pyrope. American Mineralogist, 76, 49–59.

Geiger, C.A., Armbruster, T., Lager, G.A., Jiang, K., Lottermoser, W., and Amthauer, G. (1992) A combined temperature dependent ^{57}Fe Mössbauer and single crystal X-ray diffraction study of synthetic almandine: Evidence for the Gol'danskii-Karyagin effect. Physics and Chemistry of Minerals, 19, 121–126.

Geller, S. (1967) Crystal chemistry of the garnets. Zeitschrift für Kristallographie, 125, 1–47.

Haselton, H.T., Jr. and Westrum, E.F., Jr. (1980) Low-temperature heat capacities of synthetic pyrope, grossular, and $pyrope_{60}grossular_{40}$. Geochimica et Cosmochimica Acta, 44, 701–709.

Hofmeister, A.M. and Chopelas, A. (1991) Vibrational spectroscopy of end-member silicate garnets. Physics and Chemistry of Minerals, 17, 503–526.

Hsu, L.C. (1968) Selected phase relations in the system Al-Mn-Fe-Si-O-H: A model for garnet equilibria. Journal of Petrology, 9, 40–83.

Huebner, J.S. (1971) Buffering techniques for hydrostatic systems at elevated pressures. G.C. Ulmer, Ed., Research Techniques for High Pressure and High Temperatures, p. 123–177. Springer-Verlag, New York.

Hummel, W., Hauser, J., and Bürgi, H.B. (1991) Peanut: Computer graphics program to represent atomic displacement parameters. Journal for Molecular Graphics, 8, 214–220.

Kolesov, B.A. and Geiger, C.A. (1997) Roman spectra of silicate garnets. Physics and Chemistry of Minerals, in press.

Matthes, S. (1961) Ergebnisse zur Granatsynthese und ihre Beziehungen zur natürlichen Granatbildung innerhalb der Pyralspit-Gruppe. Geochimica and Cosmochimica Acta, 23, 233–294.

Meagher, E.P. (1975) The crystal structures of pyrope and grossularite at elevated temperatures. American Mineralogist, 60, 218–228.

Menzer, G. (1928) Die Kristallstruktur der Granate. Zeitschrift für Kristallographie, 69, 300–396.

Merli, M., Callegari, A., Cannillo, E., Caucia, F., Leona, M., Oberti, R., and Ungaretti, L. (1995) Crystal-chemical complexity in natural garnets: structural constraints on chemical variability. European Journal of Mineralogy, 7, 1239–1249.

Mottana, A. (1974) Melting of spessartine at high pressure. Neues Jahrbuch für Mineralogie, Monatshefte, H6, 256–271.

Novak, G.A. and Gibbs, G.V. (1971) The crystal chemistry of the silicate garnets. American Mineralogist, 56, 791–825.

Ottonello, G., Bokreta, M., and Sciuto, P.F. (1996) Parameterization of energy and interactions in garnets: End-member properties. American Mineralogist, 81, 429–447.

Prandl, W. (1966) Verfeinerung der Kristallstruktur des Grossulars mit Neutronen- und Röntgenstrahlbeugung. Zeitschrift für Kristallographie, 123, 81–116.

Quartieri, S., Antonioli, G., Artioli, G., Geiger, C.A., and Lottici, P.P. (1997) A temperature dependent X-ray absorption fine structure study of dynamic X-site disorder in almandine: A comparison to diffraction data. Physics and Chemistry of Minerals, in press.

Rossman, G.R. and Aines, R.D. (1991) The hydrous components in garnets: Grossular-hydrogrossular. American Mineralogist, 76, 1153–164.

Shannon, R.D. (1976) Revised effective ionic radii and systematic studies of interatomic distances in halides and chalcogenides. Acta Crystallographica, A32, 751–767.

Siemens (1990) SHELXTL PC 4.1. Siemens Analytical X-ray Instruments, Madison, Wisconsin.

Skinner, B.J. (1956) Physical properties of end-members of the garnet group. American Mineralogist, 41, 428–436.

Snow, R.B. (1943) Equilibrium relationships on the liquidous surface in part of the $MnO\text{-}Al_2O_3\text{-}SiO_2$ system. Journal of the American Ceramic Society, 19, 11.

Watson, E.S., O'Neill, M.J., Justin, J., and Brenner, N. (1964) A differential scanning calorimeter for quantitative differential thermal analysis. Analytical Chemistry, 36, 1233–1238.

Zemann, J. (1962) Zur Kristallchemie der Granate. Beiträge zur Mineralogie und Petrographie, 8, 180–188.

Zucker, U.H., Perenthaler, E., Kuhs, W.F., Bachmann, R., and Schulz, H. (1983) PROMETHEUS: A program system for investigation of anharmonic thermal vibrations in crystals. Journal of Applied Crystallography, 16, 358.

Manuscript received September 3, 1996
Manuscript accepted March 14, 1997